

Influence of Laser Linewidth and Modulation Level for Coherent Optical OFDM with Punctured LDPC Codes

Chang-Jun Ahn †, Takeshi Kamio ‡, Hisato Fujisaka ‡, and Kazuhisa Haeiwa ‡

† Department of Electrical and Electronic Engineering

Chiba University

1-33 Yayoi, Inage, Chiba 263-8522 JAPAN

‡ Department of System Engineering

Hiroshima City University

3-4-1 Ozuka-Higashi, Asaminami, Hiroshima, 731-3194, JAPAN

junny@m.ieice.org †

Abstract: - Recently, coherent optical OFDM (CO-OFDM) has been proposed for optical networks to combat chromatic dispersion. CO-OFDM system has been successfully processed and recovered for transmitted signals without optical chromatic dispersion compensation. However, in optical links, the available optical power is limited due to fiber nonlinearity, and power consumption. As previously reported, we focused on the minimizing the optical power and have proposed CO-OFDM with punctured LDPC codes and variable amplitude block codes to overcome the above-mentioned problems. In this paper, we focus on the implementation of the proposed CO-OFDM and evaluate the influence of laser linewidth and modulation level for coherent optical OFDM with punctured LDPC codes.

Key-Words: - OFDM, LDPC, RCPC codes, Puncturing codes, linewidths

1 Introduction

All light sources used for optical fiber transmission emit light, not at a single wavelength λ , but in a band of spectral width $\Delta\lambda$, distributed around λ . The speed at which light travels through a fiber depends on its wavelength and on the design of the fiber. Thus some wavelengths of the band of which the pulse is comprised may be delayed with others, leading to pulse spreading with time after traveling a significant length of fiber. In a positive dispersion fiber, short wavelengths arrive before long wavelengths, pulse spreading occurs. In optical fiber links, electronic dispersion compensation (EDC) can adaptively compensate for chromatic dispersion. Particularly, in electronic predistortion, a digital processor calculates the predistorted optical signal waveform that will become a perfect waveform at the receiver. However, predistortion requires a reverse feedback path. This means that rapid variations caused by thermal drift, mechanical vibration, optical network switching, and polarization rotation cannot be compensated [1].

Orthogonal frequency division multiplexing (OFDM) is attractive and widely studied in recent RF wireless communication systems [2], [3]. Since the signals are transmitted in parallel by using many subcarriers that are mutually orthogonal and the corresponding spectrum is shaped like rectangle, OFDM can achieve high frequency efficiency and

high data rate. Moreover, OFDM has been chosen for several broadband WLAN standards like IEEE802.11a, IEEE802.11g and European HIPERLAN/2, and terrestrial digital audio broadcasting (DAB) and digital video broadcasting was also proposed for broadband wireless multiple access systems, such as IEEE802.16 wireless MAN standard and interactive DVB-T [4], [5].

In OFDM systems, the effect of multipath channel is mitigated since it eliminates ISI by inserting guard interval longer than the delay spread of the channel. By using this feature, coherent optical OFDM (CO-OFDM) has been studied in optical network to combat chromatic dispersion [6]. The CO-OFDM system has been successfully processed and recovered for transmitted signals without chromatic dispersion compensation. Furthermore, error correction coded CO-OFDM can be increased the system performance. Since it is recognized that power efficiency of LDPC codes increases greatly with the code length, it might be advantageous to use CO-OFDM when such coding schemes like LDPC codes are used as component codes. As we all know, the characteristics of communication channel is actually changed because of the variation of environment. Therefore, it is necessary to adapt the code rate according to channel conditions. Rate-compatible punctured code (RCPC) is such an

efficient and flexible scheme that it uses a single code which can be punctured in rate compatible fashion across a range of code rate [7]. The idea of RCPC has been applied to various codes, such as convolution codes [7], turbo codes [8] and LDPC codes [9]. Among them, LDPC codes have more freedom in choosing puncturing patterns. In [9], Ha *et al.* proposed an efficient method to determine good puncturing patterns by linear programming. Moreover, they also show that punctured codes have small performance degradation compared with the threshold. However, in optical links, the available optical power is limited due to safety and power consumption.

As previously reported, we focused on the minimizing the optical power and have proposed CO-OFDM with punctured LDPC codes and variable amplitude block codes [10]. For minimizing the required bias in optical fiber links, we consider the RCPC without erasing the coded bits corresponding to zeros with puncturing patterns and assign them to the subcarrier. In this case, the transmission rate is not degraded compared with the original code with reducing the transmitted power. In this paper, we focus on the implementation of the proposed CO-OFDM and evaluate the influence of laser linewidth and modulation level for coherent optical OFDM with punctured LDPC codes. This paper is organized as follows. The system model is described in Section 2. In Section 3, we show the computer simulation results. Finally, the conclusion is given in Section 4.

2 System model

2.1 Rate-compatible LDPC codes

For the puncturing problem, bit nodes of a bipartite graph can be grouped in accordance with their degrees. Thus, all coded symbols have the same degree in a group denoted by G_j where $2 \leq j \leq d_{l,max}$.

We shall randomly puncture a proportion π_j^0 of the symbols in G_j , where π_j^0 is determined in a systematic way to optimize performance. Here, $p^{(0)}$ is the total puncturing fraction, namely $p^{(0)} = (\text{the number of punctured bit nodes}) / (\text{the number of bit nodes})$. We extend the distribution pair, $(\lambda(x), \rho(x))$, to include a puncturing distribution, which is $(\lambda(x), \rho(x), \pi^0(x))$, where $\pi^0(x) = \pi_2^0 x + \pi_3^0 x^2 + \dots + \pi_{d_{l,max}}^0 x^{d_{l,max}}$ and $0 \leq \pi_j^0 \leq 1$. The puncturing fraction, $p^{(0)}$ is expressed as

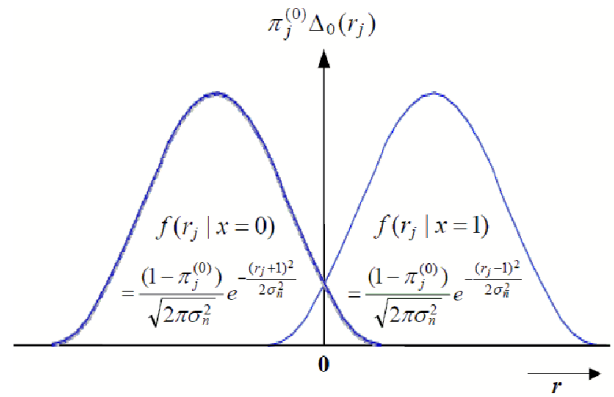


Figure 1: Channel model for the coded symbols in G_j , π_j^0 is a puncturing proportion, r_j is a received symbol, x is a message in $\{0,1\}$ which is mapped to a channel symbol in $\{-1,1\}$ and σ_n is the standard deviation of white Gaussian noise.

$$p^{(0)} = \sum_{j=2}^{d_{l,max}} \lambda_j' \pi_j^0, \quad (1)$$

where $\lambda_j' = \lambda_j / \sum_{i=2}^{d_{l,max}} \lambda_i \epsilon / \epsilon$ is the fraction of bit nodes of degree j . The symbols in G_j is shown in Fig. 1, where π_j^0 proportion of the symbols in G_j are punctured. The code optimization is to design a distribution π_j^0 for $0 \leq j \leq d_{l,max}$, which minimizes the SNR threshold for a given puncturing fraction $p^{(0)}$. An equivalent optimization, and the one implemented to find π_j^0 , is to fix the SNR threshold and maximize the puncturing fraction $p^{(0)}$. We assume that an original (unpunctured) code has been designed for rate R . Since the punctured version of that code has rate $R' > R$, its SNR threshold is higher. So rather than fix the puncturing fraction, we fix the target SNR threshold of the punctured code and optimize (maximize) the puncturing fraction $p^{(0)}$ for that threshold. As a result, a sequence of punctured codes that have thresholds close to those of codes optimally designed for the rates. The asymptotical performances of punctured LDPC codes are analyzed with Gaussian Approximation [9]. For the bit nodes in G_j , the probability density of the log-likelihood ratio (LLR) message can be expressed as

$$f(v_j) = \frac{1 - \pi_j^0}{\sqrt{4u_0}} \exp\left(-\frac{(v_j \pm m_{u_0})^2}{4m_{u_0}}\right) + \pi_j^0 \Delta_0(v_j), \quad (2)$$

$$= g^0(v_j) + \pi_j^0 \Delta_0(v_j)$$

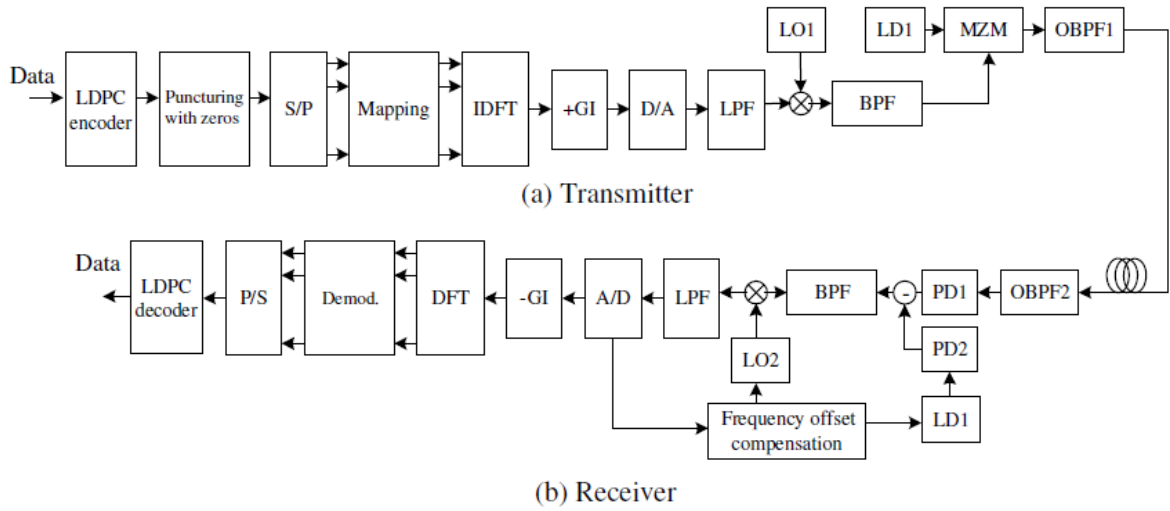


Figure 2: A block diagram of the proposed coherent optical OFDM system.

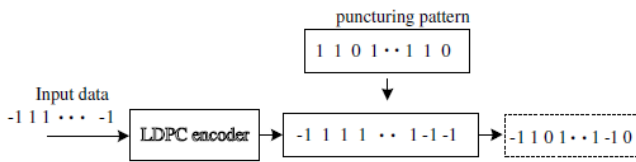


Figure 3: Puncturing for the proposed CO-OFDM system.

where $v_j = \log_2[p(r_j | x=1)/p(r_j | x=0)]$, $m_{u_0} = E[v_j | v_j \neq 0]$
 $= E[2r_j / \sigma_n^2 | r_j \neq 0]$, $\text{Var}(v_j | v_j \neq 0) = 2m_{u_0}$, π_j^0 is the
 random puncturing proportion of the coded symbols
 in G_j , and $\Delta_x(v_j) = \delta(v_j - x)$ is a shifted delta
 function.

2.2 CO-OFDM system with punctured LDPC codes and variable amplitude block codes

The transmitter block diagram of the CO-OFDM system with punctured LDPC codes and variable amplitude block codes is shown in Fig. 2(a). Firstly, the LDPC coded binary information data sequence is generated and punctured without erasing the coded bits corresponding to zeros with puncturing patterns. In general, RCPC coded systems erase the coded bits corresponding to zeros in the puncturing pattern and does not assign them to the subcarriers. Therefore, total transmission rate can be increased [7], [12]. For minimizing the required bias in optical fiber links, we

consider the RCPC coding without erasing the coded bits corresponding to zeros in the puncturing table and assign them to the subcarrier as shown in Fig. 3. In this case, the transmission rate is not degraded compared with the original code. Here, the original code means LDPC code with rate of 1/2 (1080 × 540). Moreover, the coded bits corresponding to zeros in the puncturing pattern are mapped with reduced amplitude compared with the original coded bits. The proposed CO-OFDM transmit signal can be expressed in its equivalent baseband representation as

$$s(t) = \sum_{i=-\infty}^{\infty} g(t - iT) \left\{ \sqrt{\frac{2S}{N_c}} \sum_{k=0}^{N_c-1} d(k, i) \exp[j2\pi(t - iT) \frac{k}{T_s}] \right\}, \quad (3)$$

where N_c is the number of subcarriers, T_s is the effective symbol length, S is the average transmitting power, T is the OFDM symbol length, respectively. The frequency separation between adjacent orthogonal subcarriers is $1/T_s$ and can be expressed, by using the k th subcarrier of the i th modulated symbol $d(k, i)$. The guard interval T_g is inserted in order to combat the chromatic dispersion, and hence, we have

$$T = T_s + T_g. \quad (4)$$

In Eq. (3), $g(t)$ is the transmission pulse given by

$$g(t) = \begin{cases} 1 & \text{for } -T_g \leq t \leq T \\ 0 & \text{otherwise} \end{cases} \quad (5)$$

The receiver structure is illustrated in Fig. 1(b). By applying the DFT operation, the received signal $r(t)$ is resolved into N_c subcarriers. The received signal in the equivalent baseband representation can be expressed as

$$r(t) = \int_{-\infty}^{\infty} h(\tau, t) s(t - \tau) d\tau + n(t), \quad (6)$$

where $n(t)$ is additive white Gaussian noise (AWGN). The received signal for k th subcarrier $r(k, i)$ is given by

$$\begin{aligned} r(k, i) &= \frac{1}{T_s} \int_{iT}^{iT+T_s} r(t) \exp[-j2\pi(t - iT)\frac{k}{T_s}] dt \\ &= \frac{1}{\sqrt{N_c}} \sum_{e=0}^{N_c-1} d_m(e, i) \frac{1}{T_s} \int_0^{T_s} \exp[j2\pi(e - k)\frac{t}{T_s}] \\ &\quad \left\{ \int_{-\infty}^{\infty} h(\tau, t + iT) g(t - \tau) \exp(-2\pi e \tau / T_s) d\tau \right\} dt \\ &\quad + n(k, i) \end{aligned} \quad (7)$$

where $n(k, i)$ is AWGN noise. Assuming that the maximum chromatic dispersion among subcarriers τ is shorter than the guard interval T_g , the integral with respect to τ becomes, from Eq. (5),

$$\begin{aligned} &\int_{-\infty}^{\infty} h(\tau, t + iT) g(t - \tau) \exp(-2\pi e \tau / T_s) d\tau \\ &= \int_0^{T_s} h(\tau, t + iT) \exp(-2\pi e \tau / T_s) d\tau \\ &= H(e / T_s, t + iT). \end{aligned} \quad (8)$$

Assuming that $\varepsilon_i(t)$ remains almost constant over the symbol length T_s

$$\varepsilon_i(t + iT) \approx \varepsilon_i(iT) \quad (9)$$

and hence, we have

$$H(k / T_s, iT) \approx H(k / T_s, iT), \quad \text{for } 0 \leq t \leq T. \quad (10)$$

As a result, Eq. (7) can be rewritten as

$$\begin{aligned} r(k, i) &\approx \frac{1}{T_s} \sqrt{\frac{2S}{N_c}} \sum_{e=0}^{N_c-1} d(e, i) \cdot \int_0^{T_s} \exp[j2\pi(e - k)t / T_s] \\ &\quad \cdot \left\{ \int_{-\infty}^{\infty} h(\tau, t + iT) g(t - \tau) \exp(-2\pi e \tau / T_s) d\tau \right\} dt \\ &\quad + n(k, i) \\ &= \sqrt{\frac{2S}{N_c}} H(k / T_s, iT) d(k, i) + n(k, i). \end{aligned} \quad (11)$$

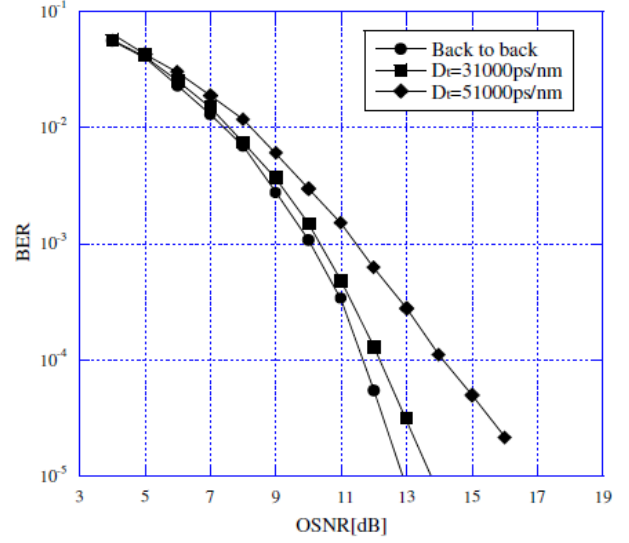


Figure 4: BER of the CO-OFDM for various cumulative chromatic dispersion D_t with QPSK and the laser linewidth of 100KHz.

In Eq. (11), we can rewrite the H due to up- and down-optical converter as

$$H(k / T_s, iT) \approx e^{j(\phi_{LD1} - \phi_{LD2})} \cdot e^{j\xi_d(k / T_s)} \quad (12)$$

where ϕ_{LD1} , ϕ_{LD2} are the phase noise due to the laser diode 1 and 2 (LD1, LD2), $\xi_d(k / T_s)$ is the phase dispersion for each subcarrier due to the fiber chromatic dispersion, and $\xi_d(k / T_s) = \pi c D_t (f_k / f_{LD1})^2$ where f_{LD1} and f_k are the frequency of subcarrier and optical carrier, D_t is total chromatic dispersion, respectively. The system is simply a linear channel with a constant phase shift $\xi_d(k / T_s)$ as far as each individual subcarrier k is concerned. This constant phase will be automatically included in symbol decision on the individual subcarrier basis, resulting in superior dispersion tolerance for CO-OFDM format. The receiver decides the amplitude values only to ± 1 in the proposed system, while ± 1 and 0 are used as the transmitted amplitude value.

3 Computer Simulated Results

In the simulation, we have used symbol period of 25.6ns, guard interval of 3.2ns, and number of subcarriers of 256. QPSK and 16QAM are used for each subcarrier resulting in total bit rate of 20Gbit/s and 40Gbit/s. The linewidth of LD1 and LD2 is assumed to be 100 KHz each, which is close to value achieved with commercially available semiconductor lasers. Moreover, we also consider the laser linewidth of 1MHz. The link optical noise from the optical

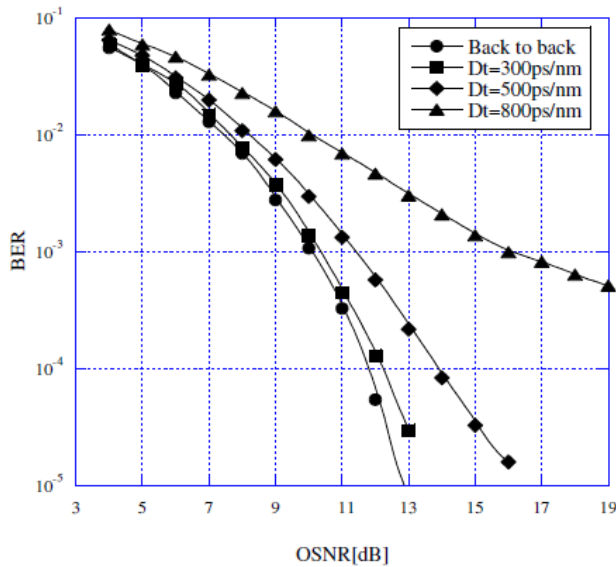


Figure 5: BER of the CO-OFDM for various cumulative chromatic dispersion D_t with QPSK and the laser linewidth of 1MHz.

amplifiers is assumed to be white Gaussian noise and the phase noise of the laser is modeled as white frequency noise characterized by its linewidth [6]. In this paper, the fiber nonlinearity is not considered and optical filters are ideal in rejecting outband interference. Moreover, OFDM window synchronization is assumed to be perfect.

The data stream is encoded. Here, LDPC codes (rate $r=1/2$, 1080×540) are used. The coded bits are punctured and QPSK and 16QAM modulated, and then the pilot signal and data signal are multiplexed. The OFDM time signals are generated by an IDFT and cyclic extensions have been inserted to combat chromatically dispersion. In the receiver, the received signals are erased the guard interval and S/P converted. The parallel sequences are passed to an DFT operator, which converts the signal back to the frequency domain. The frequency domain data signal is detected and demodulated. After data detection, bits are decoded by the sum-product algorithm.

Fig. 4 shows the BER of the CO-OFDM for various cumulative chromatic dispersion D_t with

TABLE 1: SIMULATION PARAMETERS.

Modulation	QPSK, 16QAM
Demodulation	Coherent detection
Symbol period	25.6 ns
Guard interval	3.2 ns
Number of carriers	$N_c = 256$
Laser linewidth	100KHz, 1MHz
LDPC code	1080×540

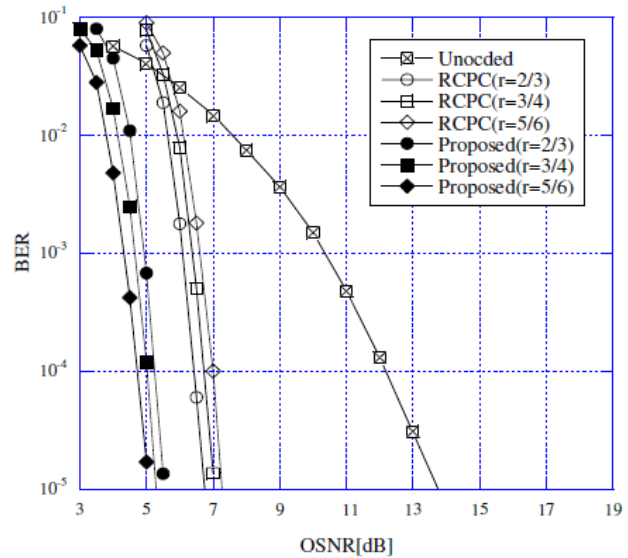


Figure 6: BER of the uncoded CO-OFDM, the RCPC coded CO-OFDM, and the proposed CO-OFDM for chromatic dispersion D_t of 31000ps/nm with QPSK and the laser linewidth of 100KHz.

QPSK and the linewidth of 100KHz. From the simulation results, the BER of the chromatic dispersion of 31000ps/nm obtains only 0.5dB penalty at BER of 10^{-4} compared with the back-to-back. Moreover, the BER of the chromatic dispersion of 51000ps/nm obtains only 2dB penalty at BER of 10^{-4} compared with the back-to-back. As a result, CO-OFDM can reduce the effect of chromatic dispersion.

Fig. 5 shows the BER of the CO-OFDM for various cumulative chromatic dispersion D_t with QPSK and the linewidth of 1MHz. From the simulation results, the BER of the chromatic dispersion of 300ps/nm with the linewidth of 1MHz obtains the approximately same as that of the chromatic dispersion of 31000ps/nm with the linewidth of 100 KHz. Moreover, by increasing the chromatic dispersion, the BER performance is significantly degraded. This is because a large linewidth results in large fiber dispersion. Therefore, the transmission distance is also degraded. To overcome this problem, a number of laser applications require lasers with a very narrow optical linewidth.

Fig. 6 shows the BER of the uncoded CO-OFDM, the RCPC coded CO-OFDM, and the proposed CO-OFDM for chromatic dispersion D_t of 31000ps/nm with QPSK and the laser linewidth of 100KHz. In general, the RCPC coded system erases the coded bits corresponding to zeros in the puncturing pattern and does not assign them to the subcarriers. Meanwhile, in the proposed system, we consider the RCPC coding without erasing the coded

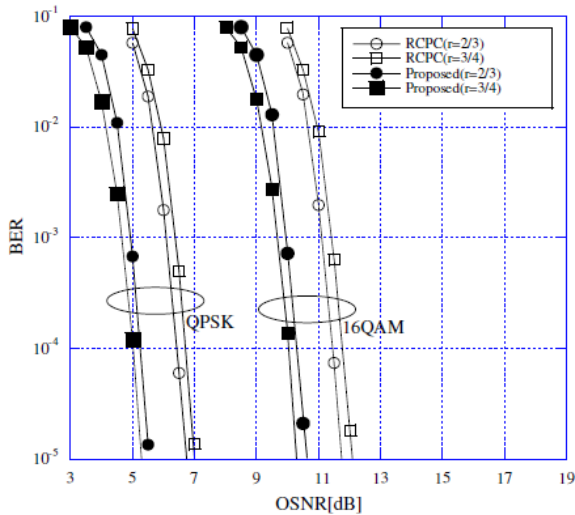


Figure 7: BER of the the RCPC coded CO-OFDM, and the proposed CO-OFDM for chromatic dispersion D_t of 31000ps/nm with QPSK, 16QAM and the laser linewidth of 100KHz.

bits corresponding to zeros in the puncturing pattern and assign them to the subcarrier. In this case, the transmission rate is not degraded compared with the original code. Moreover, the coded bits corresponding to zeros in the puncturing pattern are mapped with reduced amplitude compared with the original coded bits, and they can be decoded with the LDPC decoder. In this case, the bit rates of the proposed systems are the same as that of the original code with reducing the required OSNR. From the simulation results, it is shown that our proposed scheme with $r=5/6$ achieves 0.2dB and 0.5dB gains compared with proposed scheme with $r=3/4$ and $r=2/3$ at BER of 10^{-4} , respectively. Meanwhile, the RCPC code CO-OFDM can increase the total transmission rate compared with the original code and the proposed system. However, a large power is required to detect the received optical signals.

Fig. 7 shows the BER of the RCPC coded CO-OFDM, and the proposed CO-OFDM for chromatic dispersion D_t of 31000ps/nm with QPSK, 16QAM and the laser linewidth of 100KHz. From the simulation result, 16QAM achieves approximately the same BER property with 5dB penalty compared to QPSK. It means that the proposed CO-OFDM can easily increase the transmission rate with high modulation levels.

4 Conclusion

In this paper, we have evaluated the CO-OFDM with punctured LDPC codes and variable amplitude block

codes with various laser linewidths and modulation levels. From the simulation results, the BER of the chromatic dispersion of 300ps/nm with the linewidth of 1MHz obtains the approximately the same as that of the chromatic dispersion of 31000ps/nm with the linewidth of 100 KHz. Moreover, by increasing the chromatic dispersion, the BER performance is significantly degraded. To overcome this problem, CO-OFDM system requires lasers with a very narrow optical linewidth. Moreover, the proposed system can increase the transmission rate with high modulation levels.

References:

- [1] D. McGhan, C. Lapele, A. Savchnko, L. Chuandong, G. Mak, and M. O'Sullivan, "5120km RZ-DPSK transmission over G652 fiber at 10Gbps with no optical dispersion compensation," *Proc. of OFC 2005*, 2005, pp. 79-81.
- [2] L. Cimini, "Analysis and simulation of a digital mobile channel using OFDM," *IEEE Trans. on Comm.*, Vol. 33, 1985, pp. 665-675.
- [3] J. A. C. Bingham, "Multicarrier modulation for data transmission: an idea whose time has come," *IEEE Communications Magazine*, Vol. 28, 1990, pp.5-14.
- [4] ETSI ETS 301 958, "Digital Video Broadcasting (DVB); interaction channel for digital terrestrial television (RCT) incorporating multiple access OFDM," *ETSI, Tech. Rep.*, March 2002.
- [5] "IEEE draft standard for local and metropolitan area network-part 16: Air interface for fixed broadband wireless access systems -medium access control modifications and additional physical layers specifications for 2-11GHz," *IEEE LAN MAN Standards Committee*, 2002.
- [6] W. Shieh and C. Athaudage, "Coherent optical orthogonal frequency division multiplexing" *Electronics Letter*, Vol.42, no.10, 2006.
- [7] J. Hagenauer, "Rate-compatible punctured convolutional codes (RCPC codes) and their applications," *IEEE Transactions on Communications*, Vol. 36, 1988, pp. 389-400.
- [8] A. Barbulescu. "Rate-compatible turbo codes". *Electronic Letter*, vol.31, 1995, pp. 535-536.
- [9] J. Ha, J. Kim, and S. McLaughlin, "Rate compatible puncturing of low density parity check codes," *IEEE Transactions on Information Theory*, Vol. 50, 2004, pp. 2824-2836.
- [10] C. Ahn, S. Takahashi, H. Fujisaka, T. Kamio, and K. Haeiwa, "Power Consumption for Coherent Optical Orthogonal Frequency Division Multiplexing with Punctured LDPC Codes and Variable Amplitude Block Codes," *IEEE Journal*

of *Lightwave Technology*, Vol.26, no.14, 2008, pp.2227-2234.

- [11] T. J. Richardson, A. Shokrollahi, and R. L. Urbanke, "Design of capacity-approaching irregular low-density paritycheck codes," *IEEE Transactions on Information Theory*, Vol. 47, 2001, pp. 619-637.
- [12] L. Diana and J. M. Kahn, "Rate adaptive modulation techniques for infrared wireless communications," *Proc. of IEEE ICC99*, vol.1, 2000, pp.597-603.

University. He holds a D.Eng. Degree. In 1997, he received an Invention and Research Achievement Award from the Tokyo Metropolitan Award from the Tokyo Metropolitan Government. He also received a Development Award from the Image and Information Media Society in 1998 and an Advancement Award in 2001, IEICE member (fellow).

Biographies

Chang-Jun Ahn received the Ph.D. degree in the Department of Information and Computer Science from Keio University, Japan in 2003. From 2003 to 2006, he was with the Communication Research Laboratory, Independent Administrative Institution (now the National Institute of Information and Communications Technology). In 2006, he was on assignment at ATR Wave Engineering Laboratories. From 2007 to 2009, he was a lecturer in Hiroshima City University. Currently, he is an associate professor in Chiba University, Japan.



Takeshi Kamio received the B.E., M.E. and Ph.D. degrees from Shizuoka University, Japan, in 1994, 1996 and 1999, respectively. From 1996 to 1999, he was a Research Fellow of the Japan Society for the Promotion of Science. In 1999, he joined the Faculty of Information Sciences, Hiroshima City University. Currently, he is a lecturer in the Department of Systems Engineering. His research interests are design, learning methods, and applications of neural networks.



Hisato Fujisaka received B.E., M.E., and Dr. Eng. degrees from Keio University, Japan in 1981, 1983, and 1994, respectively. He worked in the Department of Optical Communications, Osaki Electric Co. until 1997. He is currently an associate professor in Faculty of Information Sciences, Hiroshima City University. His research interests include analysis and synthesis of nonlinear signal processing and communication circuits.



Kazuhisa Haeiwa graduated from the department of Electrical Engineering, Tokushima University. He was engaged in the design and development of broadcasting transmitters. Since 2004, he has been a professor on the Faculty of Information Science, Hiroshima City